Computational and Theoretical Chemistry 1103 (2017) 71–82

Contents lists available at ScienceDirect

Computational and Theoretical Chemistry

journal homepage: www.elsevier.com/locate/comptc

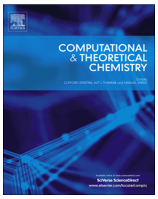

Combined DFT and NBO approach to analyze reactivity and stability of $(CuS)_n$ (n = 1–12) clusters

J. Octavio Juárez-Sánchez [a], Donald H. Galván [b], Alvaro Posada-Amarillas [a,*]

[a] Departamento de Investigación en Física, Universidad de Sonora, Blvd. Luis Encinas & Rosales, 83000 Hermosillo, Sonora, Mexico
[b] Centro de Nanociencias y Nanotecnología, Universidad Nacional Autónoma de México, 22800 Ensenada, B.C., Mexico

ARTICLE INFO

Article history:
Received 26 October 2016
Received in revised form 26 January 2017
Accepted 26 January 2017
Available online 31 January 2017

Keywords:
Copper sulfide clusters
DFT calculations
NBO analysis

ABSTRACT

Copper sulfide nanoparticles are attracting attention due to their interesting plasmonic properties, with potential applications in medicine and photocatalysis. In this work, copper sulfide clusters $(CuS)_n$, n = 1–12, are theoretically studied through DFT and Natural Bond Orbital (NBO) analysis. Initial random structures were optimized using the DFT method to obtain ground state structures. CuS clusters adopt 3-D geometries from n = 4. Layered (n = 6, 8) and hollow (n = 4, 5, 7, 9, 10, 12) structures appear in this study, the latter with copper atoms forming hollow frameworks. Reactivity descriptors are calculated and electrophilicity index is correlated to electron affinity. Charge transfer occurs in general from copper to sulfur atoms, as shown by NBO analysis. For the closed-shell $(CuS)_{6,8,10}$ clusters, stabilization energy shows that the dominant orbital interactions correspond to donor-acceptor orbitals $\sigma_{\mathrm{Cu-S}} \rightarrow n^{*}_{\mathrm{Cu}}$, $\sigma_{\mathrm{Cu-S}} \rightarrow \sigma^{*}_{\mathrm{Cu-S}}$, $n_{\mathrm{S}} \rightarrow \sigma^{*}_{\mathrm{S-S}}$, respectively. Electrostatic potential maps reveal regions of large and low electron density surrounding S and Cu atoms, respectively.

1. Introduction

Despite its negative effects on the environment, fossil fuels are still the main source of energy. For this reason, it is necessary to develop alternative energy sources that are environmentally friendly, with the sunlight as an attractive alternative to generate energy. It is a free and long-term natural resource, and available in large areas all over the world. This may be accomplished using sunlight harvesting materials (SHM) active in a broad range of the electromagnetic spectrum. However, the majority of the investigated materials to date, such as TiO_2, are only active in the UV (~6.8% of solar radiation). SHM active in the visible require an energy gap in a range from ~1.3 to ~3.0 eV, therefore, it is necessary to modify the energy gap in UV-active materials, or produce new nanomaterials possessing a band gap in this energy range.

Nowadays, the possibility of using semiconductor nanoparticles as SHM is a practical possibility due to experimental developments showing the feasibility of obtaining semiconductor nanoparticles with controlled size and shapes and unique optical properties. A promising material is nanosized copper sulfide (CuS), which has been efficiently synthesized [1] by a facile chemical method. In this work, UV–vis measurements showed an energy gap of ~2.15 eV for nanocrystals of about 10 nm, which are also known to be active as photocatalysts in the visible and near-infrared regions of electromagnetic spectrum [2]. Recent reports have demonstrated that CuS nanoparticles perform as good photocatalysts for organic molecule degradation, thus a potential application in wastewater cleaning has been envisaged [3]. A review summarizing some of the synthesis methods and applications of CuS nanoparticles has been recently reported [4].

On the other hand, because of its importance as a photocatalyst in the UV region, theoretical studies on $(TiO_2)_n$ (n = 16, 28, 38, 46, 60 and 68) clusters have been reported, performing density functional theory (DFT) calculations to analyze the geometry and electronic properties [5]. Similar studies have been conducted to analyze $(CdSe)_n$ (n = 9, 12, 16, 18, 21, 24, 28, 32 and 36) by DFT, finding relatively stable structures [6]. These results provided a motivation to perform theoretical studies on stoichiometric and non-stoichiometric copper sulfide clusters [7–10], to address the issue of finding ground state structures and, further on, to analyze reactivity and the structural stability from an atomistic viewpoint.

In particular, Juárez-Sánchez et al. reported DFT calculations to elucidate the ground state structure of semiconductor $(CuS)_n$ (n = 2–6) clusters [7]. Li et al. recently reported [8] a DFT study on the structures and electronic properties of Cu_nS (n = 1–8) clusters. They found that planar symmetry is broken after n = 2 and that the growth pattern is governed by copper atoms organized

---

* Corresponding author.
E-mail address: posada@cifus.uson.mx (A. Posada-Amarillas).

http://dx.doi.org/10.1016/j.comptc.2017.01.030
2210-271X/

in triangle arrangements. Additionally, the important role played by sulfur atom in the cluster stability was determined. On the other hand, extensive first principles studies at the MP2 level have been carried out on ligand-free $Cu_{2n}S_n$ (n = 1–6, 10) clusters [9,10]. Particularly, structural results on pentamer and decamer clusters, n = 5 and 10 respectively, indicate that covalent bonding is not significant between copper atoms, attributing this to the dispersion-like interaction of the d^{10}–d^{10} shells. However, a deeper understanding on the orbital interactions mediating cluster stability is still necessary as well as a theoretical analysis of chemical reactivity.

In this paper, we present an ab initio density functional theory study of the ground state properties of copper sulfide clusters of increasing size and 1:1 composition, $(CuS)_n$ (n = 1–12), and an NBO analysis to gain insight into the underlying electronic effects contributing to copper sulfide clusters stability. A hybrid exchange-correlation functional and a triple-ζ basis set are used for the computations. Energetical and electronic properties are presented here the latter connected to relevant reactivity indices, including molecular electrostatic potential maps and electrophilicity index for each ground state structure.

2. Computational details

The Gaussian 09 [11] code was used in all calculations to obtain the ground state structures of $(CuS)_{n=1-12}$ clusters. DFT computations were carried out by using the hybrid B3PW91 [12] exchange-correlation functional, with 20% Hartree-Fock exchange, combined with the Stuttgart-Dresden triple-ζ basis set (SDD) [13] This basis set considers 19 external electrons and an effective core potential (ECP) for Cu atoms, while for S atoms all electrons are taken into account. The combined use of hybrid functionals and ECPs in DFT calculations has proven to have a good performance in achieving the basis-set limit [14]. Moreover, our test runs showed that the selection of this ECP for Cu atoms reduces the computational time in about 60% as compared to all-electron def2-TZVP basis set. Initial structures were obtained through an in-house code, which considers distance constrictions between atoms to discard overlapping, or having small interatomic distances. Once obtained the ground state structures, vibrational frequencies were calculated to verify having reached a minimum in the potential energy surface (PES). All the final semiconductor structures presented here have real frequency normal modes. Table 1 shows the clusters minimum (ω_{min}) and maximum (ω_{max}) frequency values. The former presents a large variation with the cluster size, and the latter oscillates in a range ~380–435 cm^{-1}. Frequency values for all cluster normal modes are presented on Table SI1 in Supplementary Information. It is worth noting that to obtain ground-state cluster structures in the context of static DFT, massive runs were performed by using more than 200 clusters in each set of initial structures. For each cluster, the structure with the lowest energy and proper energy gap was singled out as the ground state structure. In our computations, multiplicity values resulted to be 2 for odd values of nuclearity and 3 for the even ones, except for the clusters with n = 6, 8, and 10, which minimized the total energy with a multiplicity value of 1. Remarkably, these are the higher-symmetry 3-D structures with well-defined planar arrangement of atoms.

The binding energy per atom (E_b) was estimated according to the expression:

$$E_b = -[E_{cluster} - n(E_{Cu} + E_S)]/N \qquad (1)$$

where $N = 2n$ is the total number of atoms in the cluster. The total energy, $E_{cluster}$, corresponds to the lowest energy obtained for a set of same size clusters, while E_{Cu} and E_S stand for the total ground state energy of copper and sulfur atoms, respectively. The binding energy per atom thus calculated gives the predicted amount of energy necessary to break bonds in the cluster, and therefore it can be used as a measure of its thermal stability. This stability stems from intramolecular interactions, and contributions from orbital interactions can be predicted through delocalization effects, *i.e.*, by means of donor-acceptor charge transfer obtained from stabilization energy calculations [15], defined as:

$$E^{(2)} = q_i \frac{F(i,j)^2}{\varepsilon_j - \varepsilon_i} \qquad (2)$$

In (2), q_i is the donor orbital occupancy, $F(i,j)$ is the off diagonal natural bond orbital (NBO) Kohn-Sham matrix, and ε_i, ε_j are diagonal elements. The interaction intensity between donor (bonding) and acceptor (antibonding) orbitals is directly related to the stabilization energy size. It is worth mentioning that the importance in understanding charge transfer processes has been recently highlighted [16], especially in quantum dot systems where confinement effects cause a strengthening in Coulomb interaction between electrons and holes. Thus, it is relevant to perform an NBO analysis to characterize charge transfer in copper sulfide clusters.

Furthermore, ionization potential (I) and electron affinity (A) are estimated by using Koopmans' approximation [17], which fairly connects these properties to the energy of frontier orbitals of the corresponding ground state geometries. Adiabatic I and A values are not calculated in this work mainly because ionized cluster structures can substantially change, on one side requiring additional computational resources in the optimization process, and on the other, making difficult to determine experimentally these quantities [18]. Thus, within this approximation, vertical I and A are used to quantify chemical potential $\left(\mu = \frac{1}{2}(I + A)\right)$, chemical hardness $\left(\eta = \frac{1}{2}(A - I)\right)$, and electrophilicity index $\left(\omega = \frac{\mu^2}{2\eta}\right)$ [19]. These descriptors may give reasonable indications on the reactivity features presented by the studied clusters. Specifically, ω is associated to the system's energy stabilization when electron charge transfer occurs from the environment [20], *i.e.*, measures the capacity of the system to accept electrons from donors. In this work, we normalized electrophilicity index with the largest calculated value set to unity to quantify the electrophilic nature of the studied copper sulfide clusters.

In our theoretical analysis of copper sulfide clusters, we have included the study of clusters' electron density regions using molecular electrostatic potential (ESP) calculations. These regions are characterized by sites of high or low electron density around the atomic species in the cluster. ESP is related to the electron density through Poisson's equation of electrodynamics, and is calculated from [21]:

$$V(\mathbf{r}) = \sum_A \frac{Z_A}{|\mathbf{r} - \mathbf{R}_A|} - \int \frac{\rho(\mathbf{r}')d\mathbf{r}'}{|\mathbf{r} - \mathbf{r}'|} \qquad (3)$$

Table 1
Minimum and maximum harmonic frequency values (in cm^{-1}) for each of the $(CuS)_n$ (n = 1–12) clusters.

n	1	2	3	4	5	6	7	8	9	10	11	12
ω_{min}	397.35	115.54	30.21	37.92	25.90	55.97	31.18	22.37	31.22	47.53	38.99	13.77
ω_{max}	397.35	379.92	376.42	419.14	424.06	383.72	435.82	395.18	426.70	423.96	421.95	397.50